DEVELOPMENT ON EARTHQUAKE RAPID REPORTING: ONE MINUTE AFTER- INTENSITY MAP, EPICENTER, AND MAGNITUDE

Ta-liang Teng[1], Yih-Min Wu[2], Tzay-Chyn Shin[2], Yi-Ben Tsai[3] and William H.K. Lee[1]

1. **Department of Earth Sciences, University of Southern California, Los Angeles, CA**
2. **Central Weather Bureau, Taipei, Taiwan, ROC**
3. **Institute of Geophysics, National Central university, Chungli, Taiwan, ROC**

ABSTRACT

This paper reports the recent progress on real-time seismic monitoring in Taiwan, particularly the real-time strong-motion monitoring by the Taiwan Central Weather Bureau telemetered seismic network (CWBSN), which is presently aiming at rapid reporting (RR) immediately after a large earthquake occurrence. If RR can be achieved before the arrival of the strong shaking, earthquake early warning (EW) will become possible. CWBSN has achieved the generation of the intensity map, epicenter and magnitude within one minute of the occurrence of a large earthquake. Both RR and EW are principally applied to large (M >>5) events; the requirement of on-scale waveform recording prompted CWBSN in 1995 to integrate strong-motion sensors (e.g., force-balance accelerometers) into its telemetered seismic monitoring system. Time-domain recursive processing is applied to the multi-channel incoming seismic signals by a group of networked personal computers to generate the intensity map. From the isoseismal contours, an effective epicenter is immediately identified that resides in the middle of the largest (usually the 100-gal) contour curve of the intensity map. An effective magnitude is also defined that can be derived immediately from the surface area covered by the largest (usually the 100-gal) contour curve. For a large event with a finite rupture surface, the epicenter and magnitude so derived are more adequate estimates of the source location and of the strength of destruction. The effective epicenter gives the center of the damage area, it stands in contrast with the conventional hypocenter location which only gives the initial point of rupture nucleation. The effective magnitude reflects more closely the earthquake damage potential, instead of the classical magnitude definition that emphasizes the total energy release. The CWBSN has achieved the above crucial source information in one minute, this time can further be reduced to better than 30 s as illustrated by the example in this paper, showing that earthquake early warning is indeed an achievable goal. The RR and EW information is electronically transmitted to users to allow rapid response, with or without further human intervention. In the aftermath of a damaging earthquake, the potential use of this information in timely emergency response cannot be overemphasized.

INTRODUCTION

In real-time seismic monitoring, we are aiming at rapid reporting (RR) immediately after a large earthquake occurrence. If RR can be achieved before the arrival of strong shaking, earthquake early warning (EW) will become possible. Since both RR and EW should only be applied to potentially damaging large events, a rapid identification of the magnitude is necessary. This calls for on-scale recordings which make it necessary that strong-motion sensors (e.g., force-balance accelerometers) be integrated into the telemetered seismic monitoring system. Taiwan has recently accomplished this integration on the CWBSN, and its progress on RR and EW is reported here.

Of crucial importance to an effective rapid response to a damaging earthquake is an early determination of the epicenter, the magnitude, and particularly the intensity map. These information items collectively constitute the essential elements in both RR and EW operations. In the aftermath of a large earthquake, further escalation of property damage and loss of lives can be averted, or at least greatly reduced, if timely emergency service and rescue missions can be dispatched to the most needy areas. Besides the large population, a modern society is sustained by a myriad of lifelines, transportation systems, power systems, and communication systems that are so complex that heavy earthquake shaking will expose all these systems to a great impact. Immediate damage assessments and emergency response measures indeed will prevent further escalation of the catastrophe. A community only has a finite capacity for emergency response, it is therefore necessary to optimize the effectiveness on the delivery of emergency response services. This optimization can be achieved by the immediate knowledge provided by RR or EW. The intensity map correlates well with the damage pattern, which naturally provides the best guides for the priority of rescue missions. During past earthquake catastrophes such as the disastrous 1976 Tangshan earthquake, or even as recently as the 1994 Northridge earthquake and the 1995 Kobe earthquake, knowledge of shaking damage has sometimes been obtained by rather haphazard methods from air surveys to surveys conducted by dispatched field parties. In worst cases, damage reports often become available as late as

hours or days after the main shock. Technological progress in remote sensing, signal processing, and data transmission has altered all this, and we should be able to obtain this shaking intensity information right from the seismic network in as short a time as possible in the real-time data processing.

A seismic computerized alert network was first discussed in concept by Heaton (1985). Besides the telemetry of on-scale waveforms, the crucial requirement that makes RR and EW work is the rapid and accurate determination of the magnitude, especially the magnitudes for large (M>> 5) events. In Japan, a method of earthquake early warning has been employed by its bullet train operation. Nakamura (1989) reports an upgraded version of the Japanese UrEDAS system that estimates the earthquake magnitude from the predominant period of the initial P-wave motion. This method cannot always work because for large events the ruptures will be large and the slip distributions will not be homogeneous, making it unlikely to always give a predominant period of the initial P-wave that is proportional to the magnitude. A moment estimation method is proposed by Toksoz et al. (1990); this generally requires an assumption of the fault depth. The actual implementation of a recursive stochastic deconvolution software for multi-channel input to get real-time moment tensor magnitude is demonstrated by Qu and Teng (1994) and Qu (1996). More software development is needed to reduce the computation time down to about 20 s in order for the method to be useful to RR and EW. Holden et al., (1989), in a report to the State of California, assess the technical and economical feasibility of an earthquake warning system in California, and Bakun (1990) writes a report on an early warning alert system for the U.S. Geological Survey. These findings are included in a National Research Council report (1991) recommending the implementation of real-time earthquake monitoring. Due to budget limitations, a large scale implementation has not taken place in the U.S. Some interesting progress is reported in a recent paper on Mexico City Seismic Alert System (Espinosa Aranda, 1995), It applies to a unique situation where the target area (Mexico City) is so far away from the source area that a delay time of as much as 70 s can be allowed for event identification, instead of only 20 - 30 s for the ordinary cases. Nonetheless, the Mexico results represent an outstanding success in earthquake early warning. Of course, as the distance becomes large, it requires a much stronger (therefore much infrequent) source to make its impact felt in the target area.

The recent upgrade of the Central Weather Bureau Seismic Network (CWBSN) in Taiwan provides a solution to this problem. Automatic P- and S-pickings and rapid least-squares inversion routines have reduced the routine epicenter determination time in Taiwan from about 30 minutes to about 60 s (Wu, 1996), this time can be further reduced by optimizing the processing hardware and software (Shin et al., 1996; Teng et al., 1996). Using amplitude data alone, Kanamori (1993) illustrates a method to a quick and rough estimate of the epicenter. He has further been working on methods for a quick (in minutes) magnitude determination (Kanamori, 1995). However, the most crucial piece of information for emergency response purposes, i.e., the shaking intensity, is generally not available until much later. This shaking intensity information will not be supplied by an epicenter, which merely represents the initial point of rupture nucleation for a large event. But the real-time monitoring of the strong ground motions can provide the desired answer. With telemetered multi-channel strong-motion input, the CWBSN is able to generate within one-minute the intensity map, the epicenter, and the magnitude of a M > 5 earthquake. This is accomplished by the CWBSN through (1) an upgrading of the telemetered seismic network to include both the weak- and strong- motion sensors, with a combined dynamic range of 166 dB from 10^{-8} g to 2 g, and (2) the use of efficient recursive seismic data processing software that parallel-processes the incoming multi-channel signals by a group of networked PCs. The use of 2 g maximum digital accelerographs in the CWBSN essentially keeps the seismic signals always on-scale. Software is written to rapidly generate the essential information for the RR and EW objectives. In this paper, a recent large event is used to illustrate the method that demonstrates the CWBSN capability of obtaining the one-minute intensity map and the associated epicenter and magnitude estimates. This capability is found to be extremely useful for the cognizant governmental agencies and public utilities, especially in an area like Taiwan where the seismicity is high and damaging earthquakes often occur (Figure 1). Software has been developed and installed on the CWBSN so that the one-minute intensity map and epicenter-magnitude information can be electronically transmitted to the cognizant governmental agencies, the public utilities, the communication and transportation systems, where desirable early emergency response operations can be triggered to mitigate further earthquake loss.

CWBSN -Real-Time Seismic Monitoring in Taiwan

Taiwan, with an area of 36,000 km^2 (approximately 10 % of California area), is situated at the junction of the Ryukyu Island Arc and the Philippine Island Arc. As the Philippine Sea Plate subducts northward under the Eurasia plate along the Ryukyu trench, and the Eurasia plate subducts eastward under the Pacific plate off the southern tip of Taiwan, the entire Taiwan island is under a NW-SE

compression with a measured slip rate as large as 7 cm/ year. Large active thrusts and strike-slip faults are distributed virtually all over the island. The seismicity in Taiwan (Figure 1) is about 3-5 times higher than that in California (Lee and Houck, 1977). A large part of the seismicity is found along the east coast and its offshore, while Taiwan population centers are developed over the western plains where occasional large events constitute a large part of the earthquake damage history. In Taiwan, the operation of a telemetered seismic network began in the early 1970s, while on-site analog seismic recordings began as early as the turn of this Century. In the late 1980s, digital telemetry and digital recording were introduced to seismic monitoring operations, however with only the conventional 3-component short-period velocity sensors. There were then two telemetered seismic networks covering the entire Taiwan region: one being the CWBSN, operated by the Central Weather Bureau; the other being the TTSN (Taiwan Telemetered Seismic Network), operated by the Institute of Earth Sciences of the Academia Sinica. In the early 1990s, the TTSN stations were integrated into a new CWBSN of a total of 75 stations, all equipped with matched 3-component Teledyne-Geotech S-13 seismometers. Figure 2 shows the present CWBSN station map. Like any standard short-period seismic network, seismograms of the CWBSN are extensively clipped for any event larger than M4. Thus these high-gain, short-period seismic networks provide little waveform information for large earthquakes, except perhaps the P-wave arrival times and the polarities.

In 1992, an important decision is made for CWBSN to add high-quality, well-calibrated force-balance accelerometers (FBA) to all CWBSN stations (Shin, 1993; Teng et al., 1994), making each station to consist of 6 components: 3-component short-period velocity sensors and 3-component acceleration sensors (FBAs). Also, an effort to develop and implement hardware and software of earthquake early warning was initiated (Lee, 1993; Lee et al., 1996). All signals of the CWBSN stations are digitally telemetered back to the Central Weather Bureau headquarters in Taipei for real-time recording and processing. To date, this addition of FBAs has been implemented at 45 CWBSN stations (shown as solid triangles in Figure 2). In continuous digital data streams, strong-motion signals are telemetered back at 16-bit, 50 sps, and velocity (S-13) signals are telemetered back at 12-bit, 100 sps, both in one-sec data packets. Design and field tests have just been completed to upgrade all 6-component data streams to be 16-bit and 100 sps. This CWBSN upgrade will be completed in 1997. Figure 3 gives the system responses of the velocity sensors (S-13) and the FBA accelerometers (A900A). The system has a combined dynamic range of 166 dB, or from 10^{-8} g to 2g in acceleration. Besides the upgraded CWBSN, the Central Weather Bureau in Taiwan has also installed 600 free-field digital strong-motion accelerographs with capability of absolute timing (Omega or GPS), and more than 40 real-time strong-motion monitoring arrays (each with 30 recording channels plus two timing channels) for buildings and bridges.

DATA AND METHOD

Figure 4 gives an example showing the quality of the CWBSN real-time FBA output for a M5 event. Based on the global strong-motion database available so far, it is believed that the CWBSN will hardly ever clip its strong-motion waveforms for even the largest earthquakes in the future. Figure 5 shows the typical integrated results of the FBA output that give the velocity and displacement traces for a M5.9 event. In the near-field of large events with high signal-to-noise ratio, the FBAs have been shown to be as effective a sensor as the broadband seismometers such as the Streckeissen STS-1 (Wald et al., 1991). While the FBA is good for near field recordings, it is not sensitive enough for recording teleseisms. Software has been developed to parallel-process all incoming signals in the CWBSN (Figure 6): a Vax system for processing the velocity (S-13) signals for conventional seismic monitoring, and a group of PCs networked into a fast parallel processing system for real-time monitoring. The latter is aiming at rapid reporting (RR) now, hopefully it will approach early warning (EW) capability in the near future (Shin et al., 1996; Lee et al., 1996).

Both RR and EW are only directed towards earthquakes large enough to cause damage, including those events large enough to inflict damage to areas well beyond the epicentral region. We shall refer to these large events as "consequential earthquakes", meaning that they are capable of inflicting significant damage on the societal well-being. Though the smaller events are valuable for scientific research, they draw no attention from RR and EW. In real terms, these consequential earthquakes refer to events of magnitude larger than perhaps M6 for RR and M7 for EW. Earthquake early warning will only work at distances more than 50 to 100 km away from the source region where there is enough delay time to allow response (Lee et al., 1996), therefore EW is especially directed towards really large earthquakes. An event much less than M7 will indeed be inconsequential at a distance of 100 km due to attenuation and geometrical spreading. In the work of both RR and EW, the ability to reliably determine earthquake location and magnitude within a time frame of tens of seconds (a time span shorter than the time required to complete a large source rupture process) has posed a difficult problem. Other methods, which are in parallel development with the

method of effective magnitude reported here, have been devised and numerically tested to determine the magnitude within the first 10 s after the P arrivals by: (1) using data from maximum displacement (fault slip), velocity and acceleration, and to calculate a total energy sum (Teng et al., 1994; Qu, 1996), and (2) a method of recursive moment tensor inversion (Qu and Teng, 1994). Some degree of success has been achieved, but the results are not definitive enough to be reported here. In the meantime, the real-time strong-motion monitoring of the CWBSN stations has opened up a new opportunity that provides a practical solution to this problem. The CWBSN has achieved RR within one minute after the event occurrence: i.e., in one minute after the first P-wave arrival time, the intensity map for a large event can be obtained, and the center of the isoseismal contours define an effective epicenter. Moreover, from the area enclosed by the 100-gal isoseismal contour curve, an empirical relationship is found that immediately gives an effective magnitude for the event.

PROCESSING, RESULTS AND DISCUSSIONS

With sufficient station density, real-time strong-motion monitoring opens up an interesting new opportunity for rapid determination of the intensity map and, immediately from which, the effective epicenter and effective magnitude. We introduce the terms of effective epicenter and effective magnitude to emphasize the damage-related nature of the these quantities that are more useful in practical applications. For a large event, the effective epicenter reflects the location of maximum destructive energy release originating from a large rupture surface below. For the purpose of earthquake rapid response, the classical point-source epicenter is quite inadequate in describing where the real damage action is. The effective magnitude reflects how extensively the destructive energy is delivered, it has different emphasis than the classical magnitude in that the latter relates to the total energy release which may not directly reflect the degree of destruction. In either case, the focal depth is not emphasized here. For a large energy release, a deep earthquake will have a much reduced impact on the society in terms of destructive energy. It will then give a reduced effective magnitude, even though far-field recordings may still yield a large magnitude in the classical sense.

Here, we give an actual example showing how RR works in a real-time monitoring strong-motion network. Figure 7 gives the strong-motion seismogram map of a M6.5 event in the northeastern Taiwan, as recorded by the telemetered strong-motion network stations (solid squares). The open circle is the effective epicenter obtained from the intensity map (to be discussed later), and the solid star is the epicenter obtained by the classical least-squares hypocenter location process. The time scale and amplitude scale are shown at the lower left corner of the figure. As waves travels outward, the amplitude drops off pretty much following the regional attenuation curves. In our case, the site effects are not too important, as most of the host stations (CWBSN high-gain short-period stations) are on rock sites. A station (ENT) near the epicenter records a PGA of nearly 0.5 g, but the strong motions attenuate pretty rapidly and drops to below 50 gal towards the northwest (near Taipei or the station TAP) and to below 10 gal towards the southwest (near Tainan or the station TAI). This shows that in Taiwan, which is in a tectonic region of modern orogeny (such as in California), the crust has a low Q with strong wave attenuation. Thus an event in eastern Taiwan of magnitude less than M7 may not be consequential to warrant EW insofar as its impact to the populous western Taiwan is concerned. For EW requires sufficient propagation delay time, during which the strong-motion amplitude may have already dropped with propagation distance to a level that is no longer damaging in the EW target area. Conventional short-period seismic networks, or even broadband stations (such as the GSN/IRIS stations) will give severely clipped waveforms for near field recording of a M7 event. Well-calibrated telemetered strong-motion networks then become very useful indeed for either RR or EW work.

Intensity Map: Figure 8 gives an example of what is actually happening as the multi-channel data streams of this large M6.5 event are coming in under real-time strong-motion monitoring. The panel on the left of Figure 8 shows the approximate wavefronts of S waves at different times after the origin time. Within about 30 sec, the PGAs of nearly all stations within 100 km of the source will have arrived in the monitoring center -- in this case, the CWBSN headquarters. We shall concentrate on this region within about 100 km from the epicenter, because most important and practical information of the earthquake will be derived from the observations in this region . The panel on the right of Figure 8 shows the multi-channel accelerograms. Only the NS components are shown in this figure, actually all 3-component data (of all 3 x 45 channels) are being recorded, processed, and shown up on the real-time monitor at the headquarters. The computer has already arranged the arriving signals according to their times of event triggering. The amplitudes are normalized to the PGA of each channel. Note that as the data stream of a strong-motion signal is coming into the computer, its PGA is tracked and updated until the PGA value reaches the maximum for that trace. The computer will take that value and place a small circle on that strong-motion trace to indicate where the PGA value

is taken. Thus all strong-motion data streams are processed and PGAs are picked as shown in the panel on the right of Figure 8. With the real-time PGA values, the computer proceeds to construct an intensity map in a specified time interval which in our case is every 5 s. Figure 9 shows a sequence of intensity maps obtained as the multi-channel digital strong-motion data streams are coming in. Panel A shows the intensity map at 10 s after the first P-wave trigger time. It is rather crude, with the strongest shaking contour being only 25 gal -- indicating that the strong motions represented by the principal part of the S-wave group have not arrived yet. At 20 s (panel B of Figure 9), the contour of the strongest shaking (80 gal) is better defined while contours in areas farther away from the source region have not yet been stabilized (again, due to the principal strong motions have not completely arrived in those areas). Panels C, D, E, and F of Figure 9 show the progressive refinements of the intensity maps at, respectively, 30, 40, 50, and 60 s after the first P-wave trigger. At 60 s, the intensity map is practically identical to the finalized version as shown in Figure 10. So, with real-time strong-motion monitoring, the intensity map is a function of time. It is important to focus our attention on the two intensity maps obtained at 20 s and 30 s. The largest and most important isoseismal contour curve (for 80-gal) has become well-defined between 20 s and 30 s. It is this largest isoseismal contour curve that carries the crucial information for the epicenter and magnitude needed for RR and EW.

Effective epicenter: We recall that any consequential earthquake of interest to RR and EW will have magnitude larger than M6.5, which will have a source dimension on the order of about 15 km. We know that the rupture initiation point -- usually indicated by the classical point-source hypocenter and obtained by a least-squares inversion process, is generally NOT the earthquake location of practical interest. Of more practical value in terms of emergency response to a damaging earthquake would be the effective epicenter which is defined to be the center of this highest isoseismal contour curve. This definition essentially place the effective epicenter right above the most energetic ruptured asperity in a fault plane below the surface. So, we argue that, between 20 s and 30 s after the first P-wave trigger, the effective epicenter is immediately known, which is located about the center of the (in the example of Figure 9) 80-gal contour curve. The location accuracy is not of practical interest here because the effective epicenter is not a point, and the classical point source location only reflects for a large event the nucleation point of a ruptured fault plane, which is not the location from where the real shaking radiation comes.

Effective Magnitude: The concept of the effective magnitude, in the sense of RR and EW applications, emphasizes the degree of total surface disturbance of strong shaking produced by a large earthquake. In areas of high seismic risk, this strong surface disturbance, of course, leads to high earthquake damage. With real-time strong-motion monitoring, we have shown above that the intensity map can be generated within one minute of a large event occurrence, and a straightforward method can be devised to get the effective magnitude immediately from the PGA isoseismal contour curve. In fact, the contour of a certain large PGA value, say 100 gal, is found to be particularly useful. For a 100-gal PGA corresponds to the intensity VII of the modified MM scale, and inside a zone of intensity VII, structural damage is becoming widespread. An empirical method is here introduced that is illustrated in Figure 11. Based on data from well-known published intensity maps and magnitudes of shallow damaging earthquakes, we have found a simple empirical relationship between the source areas covered by the 100-gal contour curve and the corresponding magnitudes of large historical earthquakes. For events larger than M5.5, it is clear in Figure 11 that the logarithm of the 100-gal source area is linearly proportional to the magnitude as shown in a semi-log plot. With this simple relationship, effective magnitude is immediately obtained as soon as the area inside the 100-gal contour curve is computed. In our example, the 80-gal PGA contour curve in Figure 10 is well defined at times between 20 s and 30 s of the first P-wave arrival as explained in Figure 9. A simple routine interpolates for the area inside the 100-gal contour curve, then the linear relationship shown in Figure 11 gives the effective magnitude. In this example, the derived effective magnitude is approximately M6.4, a value close enough to the magnitude M6.5 published later using moment tensor inversion. We note that, for the RR and EW applications, it is adequate that magnitude is determined to within about +/- 0.2 in uncertainty. Again, the effect of source depth has also been folded into the definition of the effective magnitude. For events of the same classical magnitude, say a M7, a shallow source at depth of 20 km will inflict considerable heavier damage than a deeper one at 100 km. In this sense, a M7 with source depth of 100 km will have a considerably smaller effective magnitude as its shaking impact is considerably smaller.

There should be no confusion between the classical definitions of epicenter and magnitude versus the "effective" definitions introduced here. The effective epicenter and effective magnitude are only used when RR and EW are in progress. After the earthquake rapid response period, these "effective" terms will be forgotten, and seismologists have plenty

of time thereafter to elaborate on their classical and academic studies.

Finally, there is a PC in the CWBSN system which is in charge of information dissemination. It organizes the findings and electronically transmits the information to subscribing users, who, from that point on, will execute whatever actions that are appropriate with the given RR or EW information. Figure 12 is a sample of the intensity map part of the electronic message transmitted via the e-mail in a test case. This test run has been successfully conducted for the past three months, the e-mail message carries nearly real-time the RR message from Taiwan across the Pacific to the authors in California whenever a M > 5 event occurs. In realistic situations when the CWBSN RR and EW system is approved by the authorities for routine operation, the subscribing users, such as the county and city offices of emergency services, the police departments, nuclear power plants, and any earthquake-safety-sensitive governmental and private agencies, will have to "hard-wire" their accesses to the CWBSN computer with special communication channels that will minimize or eliminate possible communication delays or breakdowns.

ACKNOWLEDGMENTS

We thank Professor Ching Yen Tsay, the Director of Taiwan Central Weather Bureau whose leadership is instrumental in much of the recent progress in observational seismology in Taiwan. Thanks are due to Yeong Tein Yeh, George Liu in the Institute of Earth Sciences, Academia Sinica; and Yu Lung Liu, Kuen Sung Liu, and many of their colleagues in the Observation Seismology Center of the Taiwan Central Weather Bureau, without their dedication, the real-time capability of the CWBSN cannot deliver the excellent data as illustrated in this paper. We also thank Hiroo Kanamori, and Egill Hauksson of Caltech Seismological Laboratory and Y. Nakamura of Japan Railways for many stimulating discussions. This research is partially funded by a Central Weather Bureau, Republic of China grant on Earthquake Early Warning and Strong-Motion Instrumentation Program and by a NSF grant EAR-9105322.

REFERENCES

Bakun, B. (1990). Early warning alert esteem, U.S. Geological Survey, Menlo Park, Public Affairs Memo.

Bolt, B. (1993). Earthquakes, Freeman and Co. p. 261.

Chang, S.w., Bray, J.D., and Seed, R.B. (1996). Engineering implications of ground motions from the Northridge earthquake, Bull. Seismol. Soc. Am., 86, No. 1, Part B, S270-S288.

Espinosa Aranda, J.M., Jimenez, A., Ibarrola, G., Alcantar, F., Aguilar, A., Inostroza, M., Maldonado, S. (1995). Mexico City Seismic alert System, Seismological Research Letters, 66, No. 6, 42-53.

Heaton, T.H. (1985). A model for seismic computerized alert network, Science, 228, 987-990.

Holden, R., Lee, R., and Reichle, M. (1989). Technical and economic feasibility of an earthquake warning system in California, California Division of Mines and Geology, Special Publ. 101.

Kanamori, H. (1993). Locating earthquakes with amplitude: Application to real-time seismology, Bull. Seismol. Soc. Am., 83, 264-268.

Kanamori, H. (1995). Quick determination of magnitude from on-line TERRAscope, California Institute of Technology, seismological Laboratory, interoffice Memorandum, August 31, 1995.

Kawase, H. and Aki, K. (1990). Topography effect and critical SV-wave incidence: possible explanation of damage pattern by the Whittier Narrows, California, earthquake of 1 October 1987, Bull. Seismol. Soc. Am., 80, No. 1, 1-22..

Lee, W.H.K. and Houck, S.T. (1977). Identifying high-seismicity regions of the world for earthquake-prediction studies, U.S. Geol. Survey Open-File Report 77-693, 134 pp.

Lee, W.H.K. (1993). A project implementation plan for an advanced earthquake monitoring system. Research Report of Central Weather Bureau, Taipei, Taiwan, R.O.C., No. 444, also as U.S. Geological Survey Open-File Report 94-004, 89 pp.

Lee, W.H.K., Shin, T.C., and Teng, T.L. (1996). Design and implementation of earthquake early warning system in Taiwan. Paper No. 2133, 11th World Conference of Earthquake Engineering, Acapulco, Mexico.

Nakamura, Y. (1989). Earthquake alarm system for Japan railways, Japanese Railway Engineering 28(4), 3-7.

National Research Council of the National Academy of Science. (1991). Real-time earthquake monitoring, Report from the Committee on Seismology (National Academy Press, Washington, D.C.)

Reagor, B. G., Stover, C.W., Algermissen, S.T., Steinbrugge, K.V., Hubiak, P., Hopper, M.G., and Barnhard, L.M. (1979) Preliminary evaluation of the distribution of seismic intensities, U.S. Geological Survey Professional Paper 1254, 251-258.

Richter, C.F. (1958). Elementary Seismology, Freeman and Co., p. 39 and p. 519.

Qu, J. (1996). Part II: Recursive stochastic deconvolution in the estimation of earthquake source parameters, Ph.D. Thesis, University of Southern California.

Qu, J. and Teng, T.L. (1994). Recursive stochastic deconvolution in the estimation of earthquake source parameters: synthetic waveforms, Physics of Earth and Planetary Interiors, Vol. 86, 301-327.

Scott, N.H. (1971). Preliminary report on felt area and intensity, U.S. Geological Survey Professional Paper 773, 153-154.

Shin, T.C. (1993) Progress summary of the Taiwan Strong Motion Instrumentation Program, Sym. Taiwan Strong Motion Instrumentation Program, 1 - 10, (in Chinese).

Shin, T.C., Tsai, Y.B., and Wu, Y.M. (1996) Rapid response of large earthquakes in Taiwan using a real-time telemetered network of digital accelerographs, Paper No. 2137, 11th World Conference of Earthquake Engineering, Acapulco, Mexico.

State Seismological Bureau "1976 Tangshan Earthquake" Editor Group, (1982). 1976 Tangshan Earthquake, Earthquake Publication Service, p. 4.

Teng, T.L., Hsu, M., Lee, W.H.K., Tsai, Y.B., Wu, F.T., Yeh, Y.T. and Liu, G. (1994). Annual Report to the Central Weather bureau on Earthquake early Warning and Implementation of the Strong Motion instrumentation Program.

Teng, T.L., Hsu, M., Lee, W.H.K., Tsai, Y.B., Wu, F.T. and Liu, G. (1996). Annual Report to the Central Weather bureau on Earthquake early Warning and Implementation of the Strong Motion instrumentation Program.

Toksoz, M.N., Dainty, A.M. and Bullit, J.T. (1990). A prototype earthquake warning system for strike-slip earthquakes, Pure and Applied Geophysics, 133(3), 475-487.

Wald, L.A., Hutton, L.K., Mori, J., Given, D.G. and Jones, L.M. (1991) The southern California Network Bulletin, January - December, 1990.

Wu, Y. M. (1996). E-mail message to W.H.K. Lee May 6, 1996.

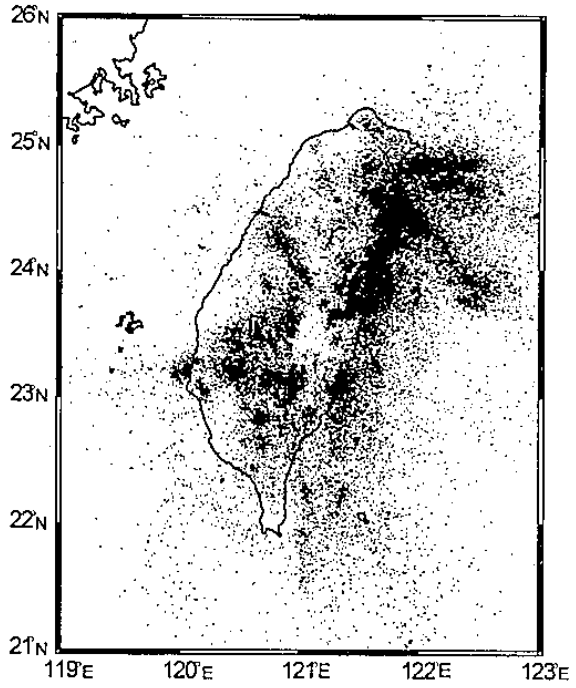

Figure 1. A Seismicity Map of Taiwan (from 1973 to 1996)

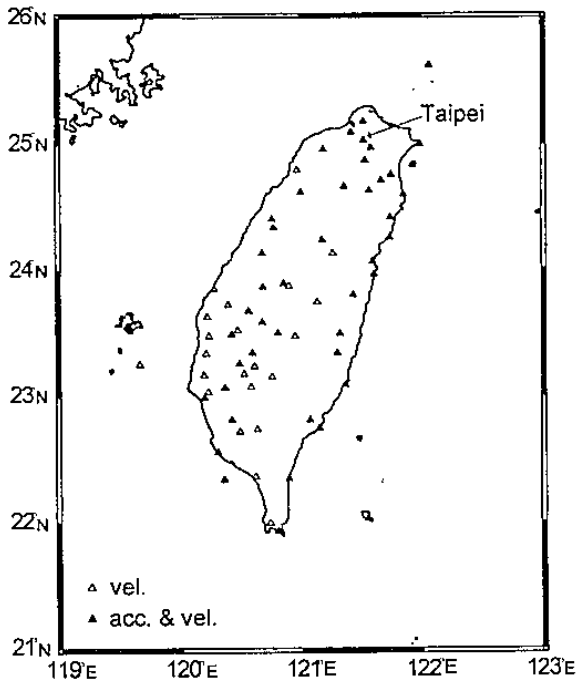

Figure 2. The CWBSN Station Map

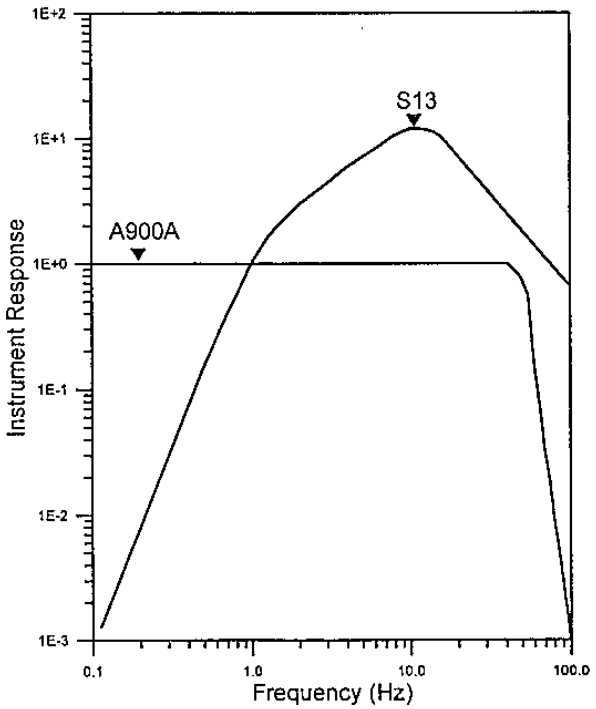

Figure 3. The System Response Curve of the CWBSN Seismic.

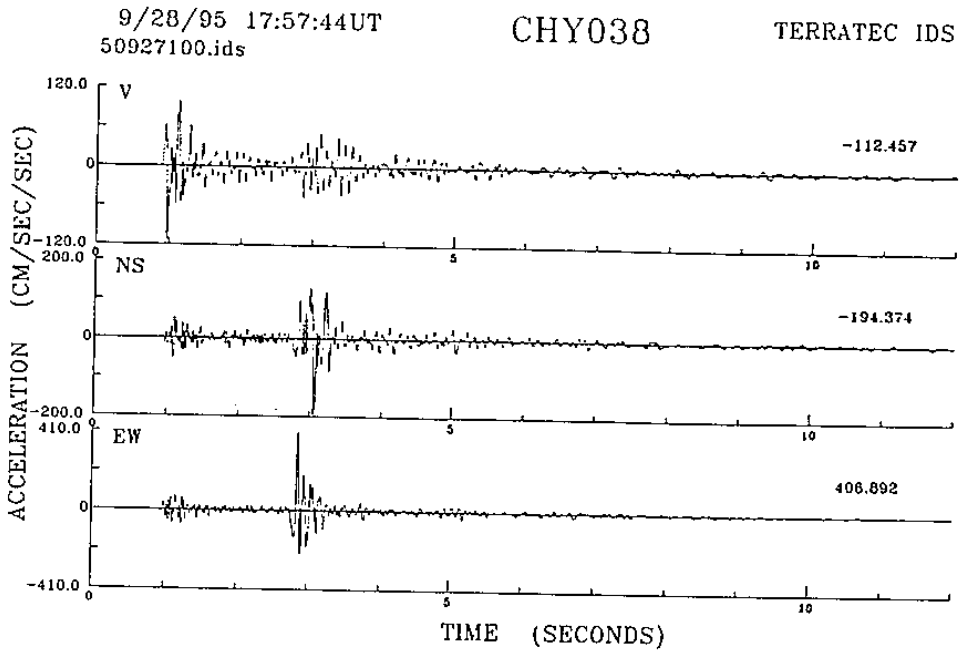

Figure 4. A Sample 3-Component Accelerograms of CWBSN.

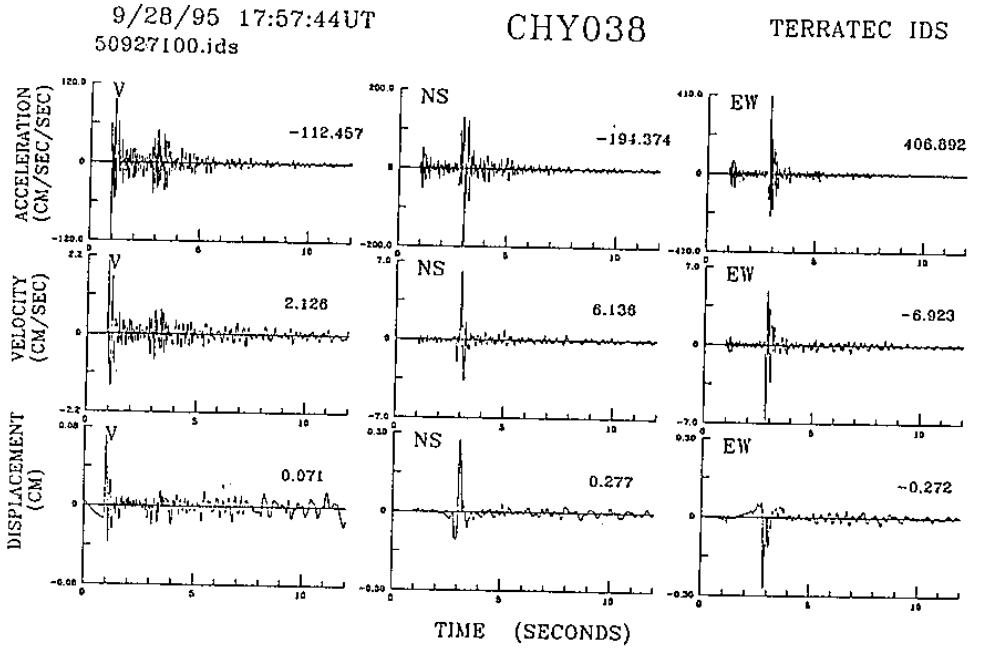

Figure 5. Velocity and Displacement Data from Recursive Integration.

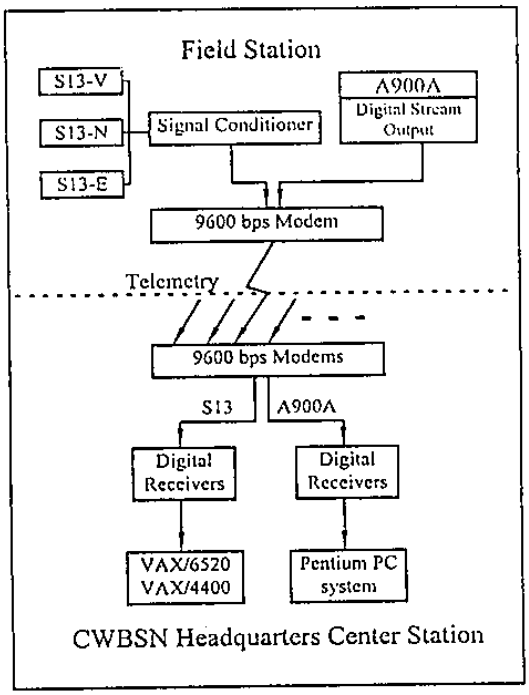

Figure 6. The Digital Telemetry Flow Chart

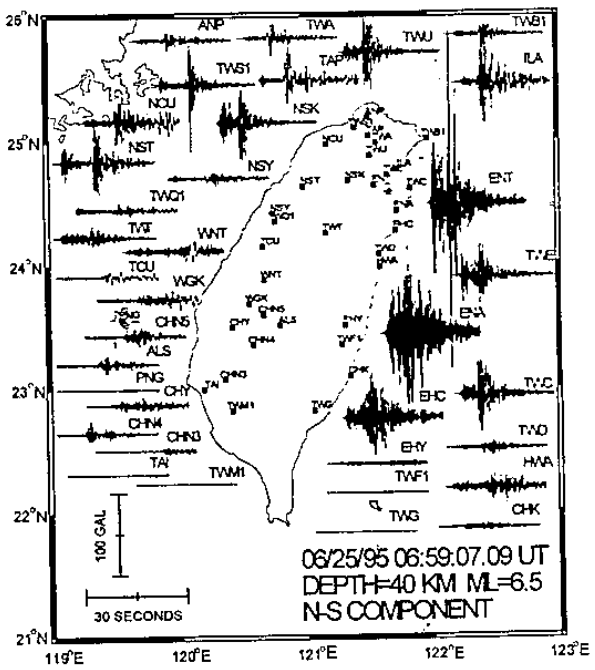

Figure 7. A Strong-Motion Seismogram Map

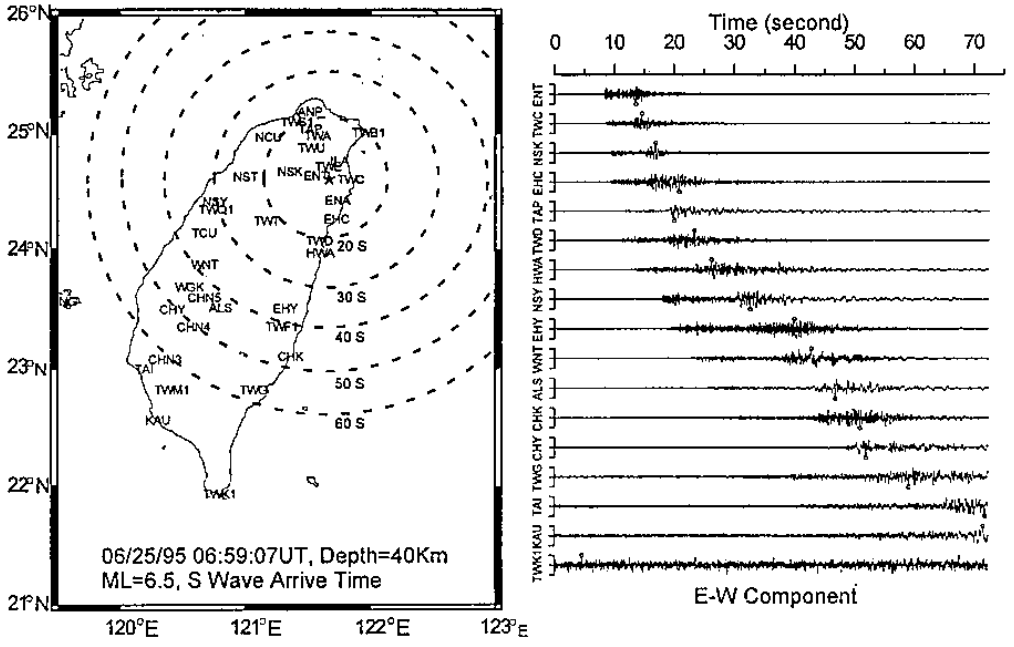

Figure 8. An Event Map Showing the Approximate 10 s Wave-fronts

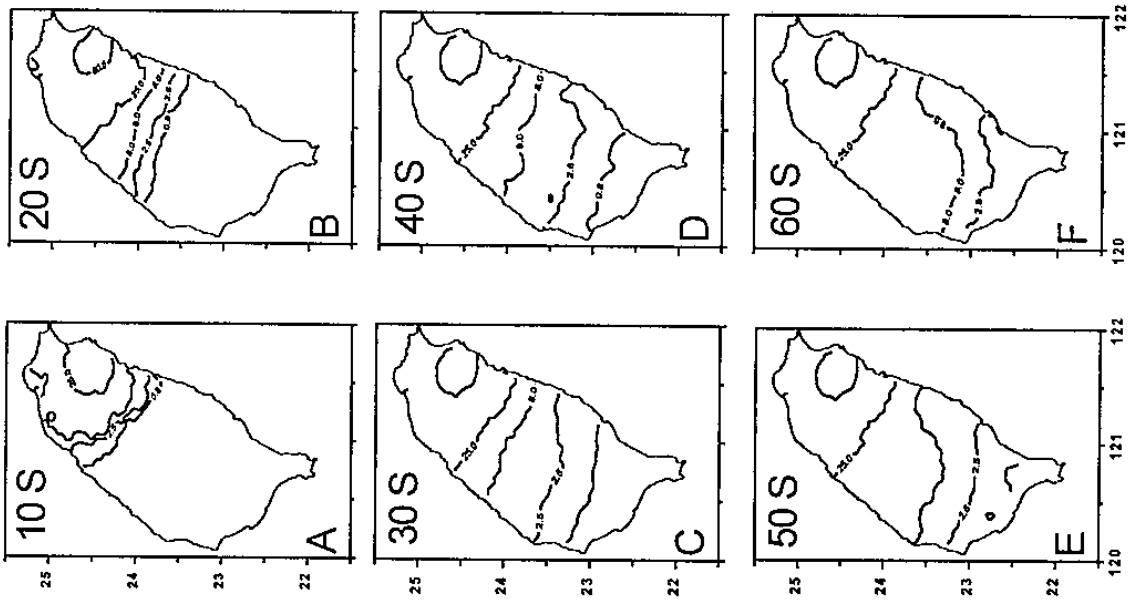

Figure 9. The Intensity Map as A Function of Time

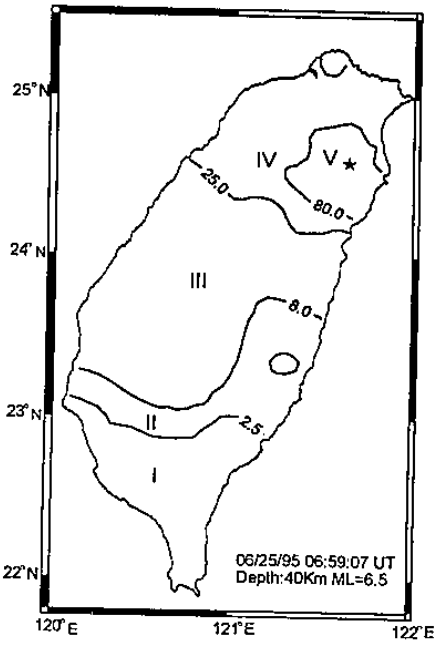

Figure 10. The Finalized Intensity Map

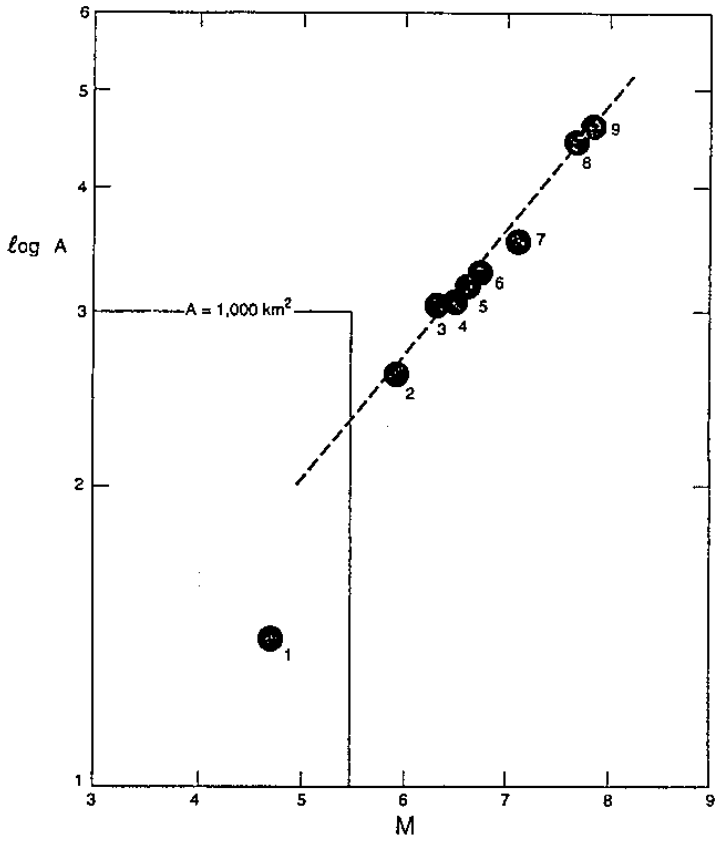

Figure 11. An Empirical Relationship between the Area Covered by the 100-gal Contour (in km²) and Earthquake Magnitude. Data compiled from:

1. Whittier earthquake, 1929 (Richter, 1958).
2. Whittier Narrow earthquake, 1987 (Kawase and Aki, 1990).
3. Long Beach earthquake, 1933 (Richter, 1933).
4. Imperial Valley earthquake, 1979 (Reagor et al., 1979).
5. San Fernando earthquake, 1971 (Scott, 1971).
6. Northridge earthquake, 1994 (Chang et al., 1996).
7. Loma Prieta earthquake, 1989 (Bolt, 1993).
8. Kern County earthquake, 1952 (Richter, 1958).
9. Tangshan earthquake, 1976 (State Seismological bureau, 1982)

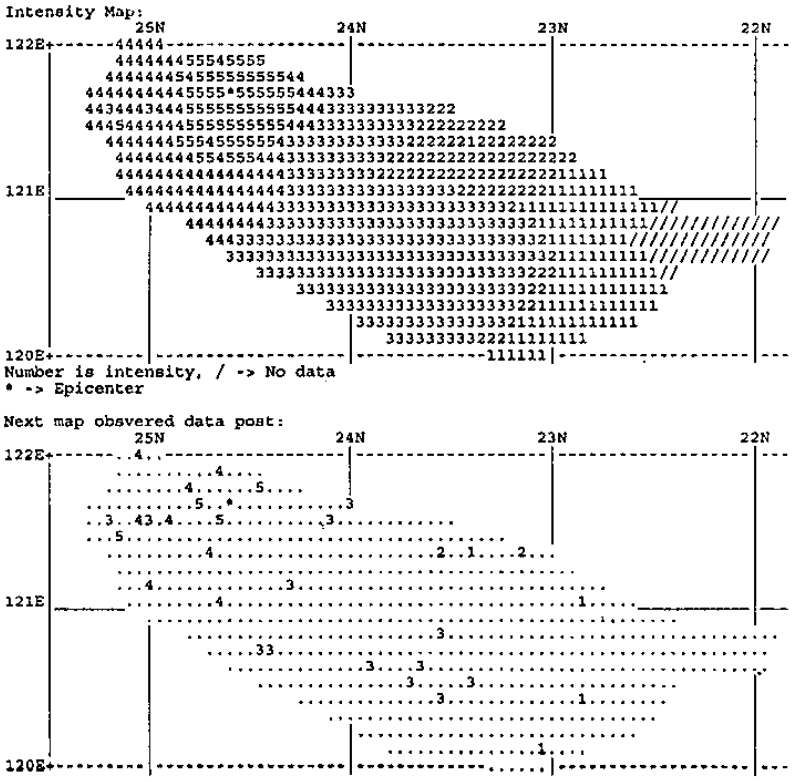

Figure 12. A Sample Output through the E-Mail: where the Intensity Map is plotted by letters, its size can be translated into area. An effective magnitude is obtained by a direct application of the empirical relationship in Figure 11.